IMPACT OF VERTICAL STRUCTURE ON PERTURBATION GROWTH

C. A. REYNOLDS and R. GELARO
Naval Research Laboratory, Monterey, CA, USA

T. N. PALMER
European Centre for Medium-Range Weather Forecasts, Reading, Berkshire, UK

For large dynamical systems, the evolution of a small initial perturbation is often examined in terms of its fastest growing component, which is the subspace defined by its projection onto the leading singular vectors. The evolution of the entire perturbation will, however, be a function of both the full growing and decaying subspaces. To explore the relationship between these subspaces, the fastest growing and fastest decaying singular vectors for a relatively small quasi-geostrophic model are examined and compared.

The leading (trailing) singular vector describes the fastest growing (decaying) linear perturbation about a nonlinear trajectory, as measured by a specified metric. The amplification factors of these perturbations are given by the corresponding singular values. (See Buizza and Palmer 1995, for a discussion of singular vectors and their relationship to other dynamical quantities.) The 3-level quasi-geostrophic model used here is described in detail in Marshall and Molteni (1993) and is forced by prescribed potential vorticity source terms corresponding to a Northern Hemisphere winter climatology. The model is small enough (1449 degrees of freedom) so that the full set of singular values and vectors can be calculated explicitly. In this study, a kinetic energy metric is used, and singular vectors are calculated for varying optimization times starting from 13 consecutive days at the end of a 113 day nonlinear integration.

Figure 1 shows the leading singular values, or amplification factors, for the 13 cases considered, for both 24 hr and 48 hr optimization times. As shown in previous studies, the amplification factor for the fastest growing perturbation exhibits considerable case-to-case variability, or flow dependence. Also shown in Fig.1 is the inverse of the trailing singular values. For a non-dissipative system, the leading singular value is approximately equal to the inverse of the trailing singular value. As dissipation is increased, the leading and trailing singular values both become smaller, so that the separation between the leading singular value and the inverse of the trailing singular value increases. Figure 1 indicates that the amplification factor of the fastest decaying perturbations also exhibits considerable flow dependence. It also appears that these two curves are well correlated for both the 24 hour and 48 hour optimization times. This may suggest a dynamical link between the fastest growing perturbation and the fastest decaying perturbation. This correlation decreases as optimization time is increased.

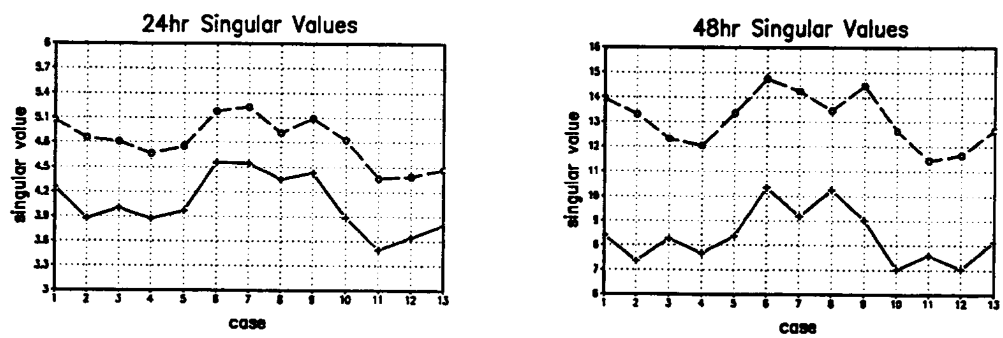

Figure 1: The leading KE singular values (amplification factors), and the inverse of the trailing KE singular values for the 13 cases examined for the 24 hr optimization time (left) and 48 hr optimization time (right). The leading singular values are indicated by crosses and the solid line, and the inverse of the trailing singular values are indicated by the circles and the dashed line. Note different scales of y axes.

The characteristics of the growing singular vectors for this model are discussed in detail in several previous studies (e.g. Molteni and Palmer 1993). In general, the fastest growing singular vectors exhibit an upward and upscale energy transfer between initial and final time. They exhibit a westward tilt with height that decreases with time as they evolve. These characteristics are contrasted with those of the fastest decaying singular vectors (Reynolds and Palmer 1998), which exhibit a downward and down-scale energy transfer between initial and final times. These decaying singular vectors have a slight eastward tilt with height at initial time that becomes more pronounced as they evolve. Quasi-geostrophic reasoning used to explain the growth of westward tilted disturbances (e.g. Holton 1979) can also be used to explain how these eastward tilted systems

would decay and become more tilted with time. In this study the spatial relationship between the leading and decaying singular vectors for a specific case is examined.

Figures 2 and 3 show the 500 mb stream-function perturbations corresponding to the fastest growing and fastest decaying KE singular vectors, respectively, at both initial and final times. Both singular vectors occur over E. Asia and the N. Pacific, in the vicinity of the strongest jet in the Northern Hemisphere. At initial time, the growing singular vector (SV1) occurs east of the decaying singular vector (SV1449). The second fastest growing and fastest decaying singular vectors (SV2 and SV1448, not shown) are in approximate quadrature (one-quarter wave length out of phase) with the singular vectors shown in Figs. 2 and 3. The third fastest growing and decaying singular vectors (SV3 and SV1447, not shown) both occur over N. America and the N. Atlantic (in the vicinity of the N. Atlantic jet).

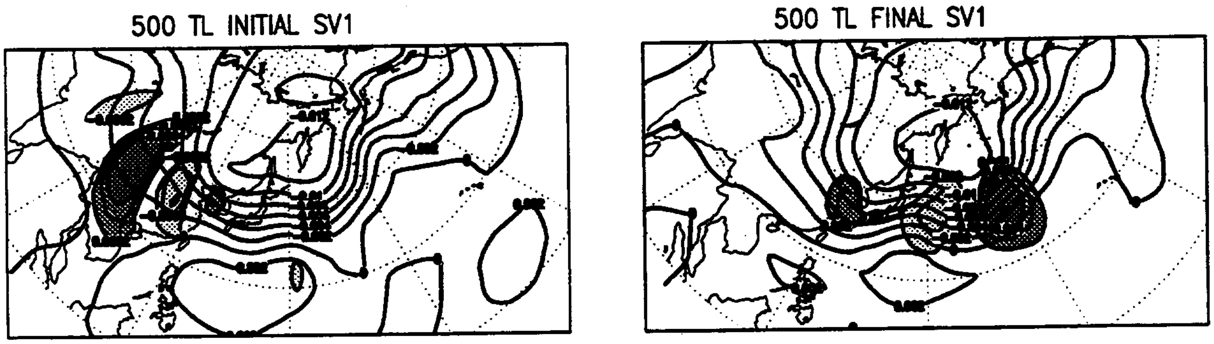

Figure 2: The 500 mb stream-function perturbation (shaded) corresponding to fastest growing KE singular vector for case 6 at initial (left) and final (right) times, superimposed upon the background 500 mb stream-function. The perturbation contour interval at final time is 10x contour interval at initial time.

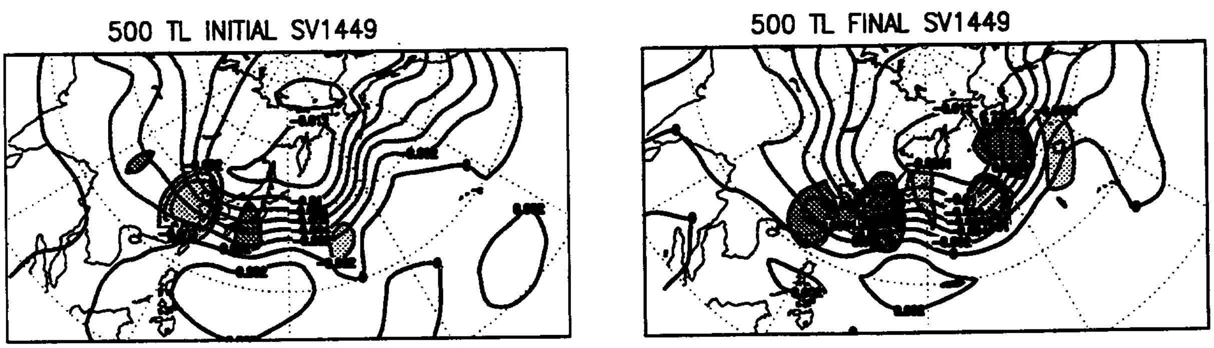

Figure 3: Same as Fig. 2 but for the fastest decaying KE singular vector. The perturbation contour interval at initial time is 20x contour interval at final time.

Figures 4 and 5 show the vertical cross-section of the stream-function perturbations at 35°N corresponding to the singular vectors shown in Figs. 2 and 3. One now sees that the perturbations are co-located at the lowest level in the model, with the growing perturbation tilted westward and the decaying perturbation tilted eastward with height. The eastward propagation speed between initial and final times is similar for both the growing and decaying modes. Similar relationships are found for the third fastest growing and decaying singular vectors over the N. Atlantic. Examination of other cases also indicates that the fastest growing and decaying singular vectors are usually co-located. When the strength of the dissipation is increased sufficiently, the structure of the decaying singular vectors changes dramatically and is characterized by global, small-scale patterns at the lowest model level. (A similar decaying singular vector to the one shown in Figs. 3 and 5 may still exist, but may not decay faster than the smallest-scale low-level patterns which are quickly damped by the model dissipation.)

The results of this preliminary study indicate that the amplification factor of the fastest decaying singular vector displays case-to-case variability similar to the amplification factor of the fastest growing singular vector. The correlations between the curves shown in Fig. 1 indicate that the fastest growing and decaying perturbations may be dynamically linked, and an examination of these vectors indicates that they are approximately co-located. This co-location occurs for other, less optimal, growing and decaying singular vectors as well. The co-location of these growing and decaying singular vectors indicates that the growth rate of initial perturbations will not only be a strong function of the local instability of the flow, but also may depend critically

on the vertical structure and tilt of the perturbation. This result has serious practical implications for operational ensemble forecasting and adaptive observations. For example, these results illustrate how the impact of extra observations on a short-term forecast will not only depend on the location of the resulting analysis increment, but also on its vertical structure. Work is on-going to examine the relationship between these growing and decaying perturbations and their nonlinear evolution, relationship to the mean flow, and dependence on optimization time and metric. The structures of analysis increments from adaptive observations and their impact on subsequent forecasts will also be examined in this context.

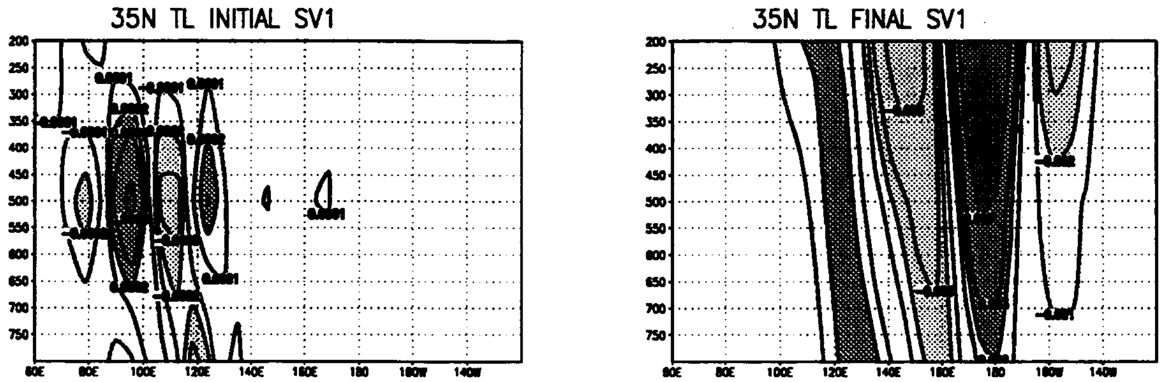

Figure 4: Vertical cross-section at 35°N of the stream-function pattern corresponding to fastest growing KE singular vector for case 6 at initial (left) and final (right) times. The contour interval at final time is 10x contour interval at initial time.

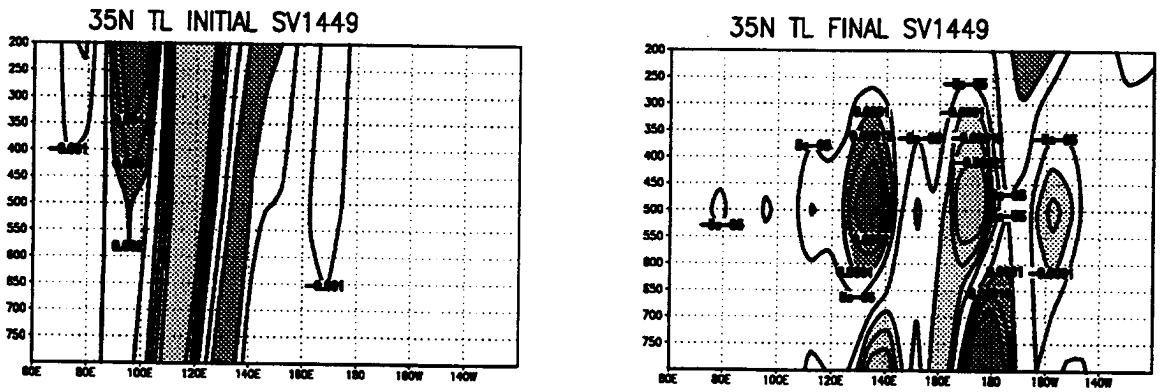

Figure 5: Same as Fig. 4 but for the fastest decaying KE singular vector. The contour interval at initial time is 10x contour interval at final time.

Acknowledgments: Support of the sponsor, Office of Naval Research, and the program manager, Naval Research Laboratory, project element 0601153N, is gratefully acknowledged.

References:

Buizza, R., and T. N. Palmer, 1995: The singular vector structure of the atmospheric general circulation. *J. Atmos. Sci.*, **52**, 1434-1456.

Holton, J. R., 1979: *An Introduction to Dynamic Meteorology, 2nd Edition.* Academic Press, Inc., Orlando, Florida, 32887

Marshal, J., and F. Molteni, 1993: Toward a dynamical understanding of planetary-scale flow regimes. *J. Atmos. Sci.*, **50**, 1792-1818.

Molteni, F., and T. N. Palmer, 1993: Predictability and finite-time instability of the northern winter circulation. *Q. J. R. Meteorol. Soc.*, **119**, 269-298.

Reynolds, C. A., and T. N. Palmer, 1998: Decaying singular vectors and their impact on analysis and forecast correction. Accepted for publication in *J. Atmos. Sci.*